Automated Fast-Flow Synthesis of Antisense Phosphorodiamidate Morpholino Oligomers

Chengxi Li[1†], Alex J. Callahan[1†], Mark D. Simon[1], Kyle A. Totaro[1], Alexander J. Mijalis[1], Nina Hartrampf[1,2], Carly K. Schissel[1], Ming Zhou[3], Hong Zong[3], Gunnar J. Hanson[3], Andrei Loas[1], Nicola L. B. Pohl[4], Bradley L. Pentelute[1,5,6,7*]

[1]Department of Chemistry, Massachusetts Institute of Technology, 77 Massachusetts Avenue, Cambridge, MA 02139, USA.

[2]Current address: University of Zurich, Department of Chemistry, Wintherthurerstrasse 190, 8057 Zurich, Switzerland."

[3]Sarepta Therapeutics, 215 First Street, Cambridge, MA 02142, USA.

[4]Department of Chemistry, Indiana University, 120A Simon Hall, 212 S. Hawthorne Drive, Bloomington, IN 47405, USA.

[5]The Koch Institute for Integrative Cancer Research, Massachusetts Institute of Technology, 500 Main Street, Cambridge, MA 02142, USA.

[6]Center for Environmental Health Sciences, Massachusetts Institute of Technology, 77 Massachusetts Avenue, Cambridge, MA 02139, USA.

[7]Broad Institute of MIT and Harvard, 415 Main Street, Cambridge, MA 02142, USA. *E-mail: blp@mit.edu

[†]These authors contributed equally to this work.

Abstract

The antisense phosphorodiamidate morpholino oligomer (PMO) drugs Eteplirsen and Golodirsen are improving the lives of some Duchenne muscular dystrophy (DMD) patients, but treating all DMD subtypes would require the development of over 50 novel antisense therapies. To rapidly prototype personalized PMO for diseases such as DMD, we designed a fully automated flow-based oligonucleotide synthesizer. Our optimized high temperature synthesis platform reduces coupling times by up to 22-fold compared to previously reported batch methods. We demonstrate the power of our new automated

28   technology with the synthesis of milligram quantities of an 18-mer reporter PMO

29   sequence in 3.5 hours, three new potential therapeutic PMO sequences targeted to exon

30   46 of the dystrophin gene in a single day, and a candidate antiviral PMO sequence

31   targeted to the SARS-CoV-2 genomic mRNA in 3.5 hours. This flexible flow synthesis

32   platform can be used for on-demand production of a broad range of personalized

33   therapeutic polymers.

34   **Introduction**

35   Phosphorodiamidate morpholino oligomers (PMO) are an important class of

36   therapeutically relevant antisense compounds[1]. Two U.S. Food and Drug Administration

37   (FDA) approved drugs, Vyondys 53[TM] (Golodirsen)[2] and Exondys 51[TM] (Eteplirsen)[3],

38   make use of the PMO backbone to treat Duchenne muscular dystrophy (DMD) (Fig. 1a).

39   Although these new antisense treatments are revolutionizing care for this difficult to treat

40   disease, more PMO drugs are required to expand this treatment strategy to all possible

41   subgroups of patients[4]. Additionally, new antivirals targeting Dengue[5], Marburg virus[6],

42   Ebola[6], and influenza[7] are in development. The PMO backbone is derived from RNA,

43   wherein the 5-membered ribosyl ring has been replaced with a 6-membered morpholinyl

44   ring and phosphate linkages have been replaced with uncharged phosphorodiamidates[1]

45   (Fig. 1b). These modifications make PMOs resistant to nucleases[8] and substantially more

46   cell permeable than RNA[9], while retaining strong binding affinity for target RNA.

47   Although PMOs are a powerful therapeutic modality, challenging synthetic

48   protocols limit their applications. Current protocols for laboratory-scale synthesis of PMOs

49   take around 3 hours for the coupling of each monomer[10], with total synthesis times on the

50   order of weeks for each sequence of interest. Furthermore, the development of a new

51   PMO therapeutic requires the synthesis of potentially hundreds of antisense sequences

52   along a gene, as sequence effectiveness is generally not known beforehand. Further lead

53   optimization cycles evolve the drug structure with sequential rounds of synthesis and

54   testing. Long syntheses of PMOs during each of these stages places a significant burden

55   on drug development timelines, that in turn limit the application of PMOs to new disease

56   types. This type of synthetic problem is not unique to PMOs; similar synthetic burdens

57   exist on the investigation of DNA analogues, and peptides/proteins. These issues have

58   largely been addressed with the development of highly efficient synthesis chemistries and

59   automated synthesizers[11,12,13,14,15].

60   We envision that the development of new antisense PMO drugs can be greatly

61   accelerated by rapid flow synthesis. We designed a new automated instrument that not

62   only eliminates repetitive human tasks, but also allows for chemical transformations not

63   feasible with manual techniques. Key to our instrument design is the use of flow chemistry

64   as it allows for precise control of reaction conditions[16]. With a thorough understanding of

65   the chemical reactions under study, a flow instrument can be improved to avoid conditions

66   otherwise conducive to the formation of side products[17, 18, 19, 20]. Combined with

67   automation, flow instruments can mix and heat reagents with efficiencies that are

68   unattainable by batch methods[21, 22, 23]. New generations of therapeutics will require rapid

69   production of drug molecules, and automated instruments are a valuable tool to address

70   these problems[24, 25].

71   In this report, we produce PMOs over an order of magnitude faster than manual

72   batch protocols with a modular automated flow synthesizer. Current automated PMO

73   synthesizers are able to only carry out reactions that already work in batch[26], but the flow

74   synthesizer we report operates at 90 °C, enhancing reaction rates to couple a new

75   nucleobase in only 8 minutes, compared to the 180 minutes typically required for a batch

76   synthesis at room temperature[10]. Including washes, total cycle time for each nucleobase

77   is 13 minutes in flow compared to 240 minutes in previous protocols[10]. Our flow protocol

78   would be challenging to replicate manually as it necessitates rapid solution changes,

79   rigorously anhydrous conditions, and the use of volatile solvents well above their boiling

80   points.

81   Using this improved methodology, we demonstrate the synthesis of PMO

82   sequences in hours instead of the weeks required if produced by traditional methods. The

83   crude quality of PMO sequences of therapeutic length obtained using the expedited

84   protocol is demonstrated to be comparable to time-consuming batch methods. We also

85   synthesized in succession three new PMO sequences targeting subtypes of DMD with no

86   current treatment options in a single day. Additionally, during the course of our research,

87   it became clear that expedited access to antisense therapeutics could become critical for

88   rapid response to new viral pathogens. As of July 2nd, 2020, a novel betacoronavirus,

89   Severe acute respiratory syndrome coronavirus 2 (SARS-CoV-2), has caused a global

90   pandemic with 10,726,802 confirmed cases and 516,970 resulting deaths[27]. Antisense

91   therapy is an attractive route for viral treatments[28], and there exists prior art into designing

92   antisense PMO treatments for the closely related Severe acute respiratory syndrome

93   coronavirus (SARS-CoV) [29, 30]. Using the reported fast flow platform, we synthesized a

94   lead PMO candidate targeted to the 5' untranslated region (UTR) of SARS-CoV-2

95   genomic mRNA in 3.5 hours. Further testing is required to determine the efficacy of the

96   new PMO sequences, but rapid flow synthesis should significantly improve lead

97   optimization cycles.
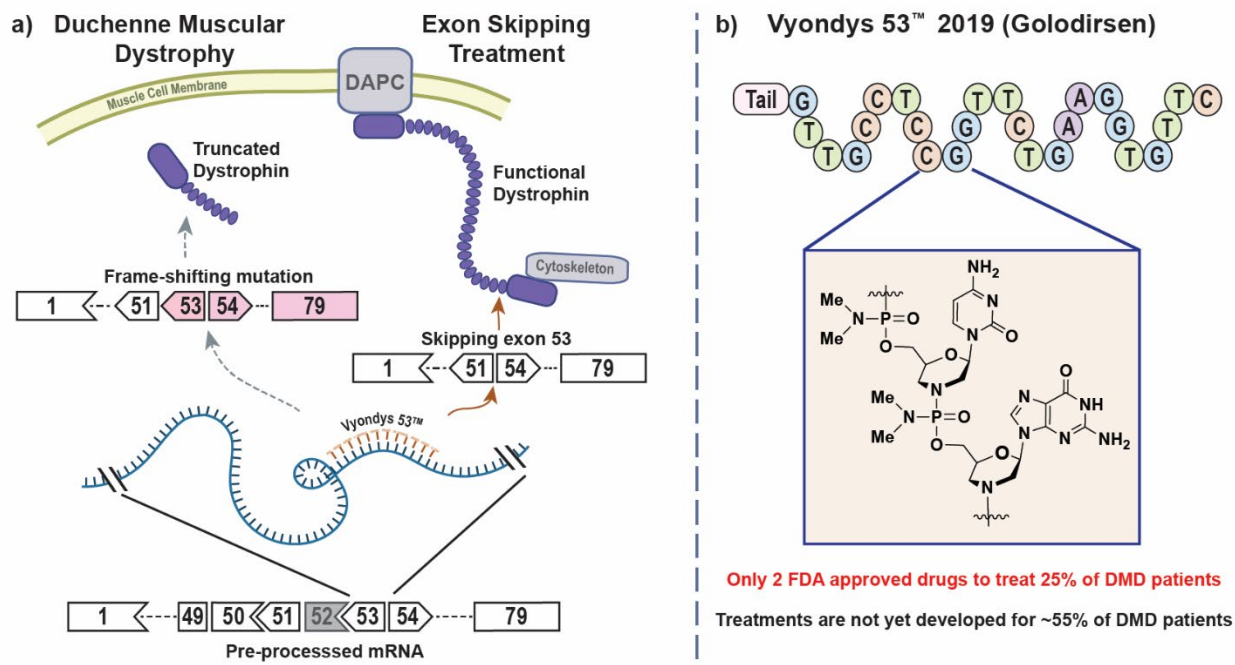
98
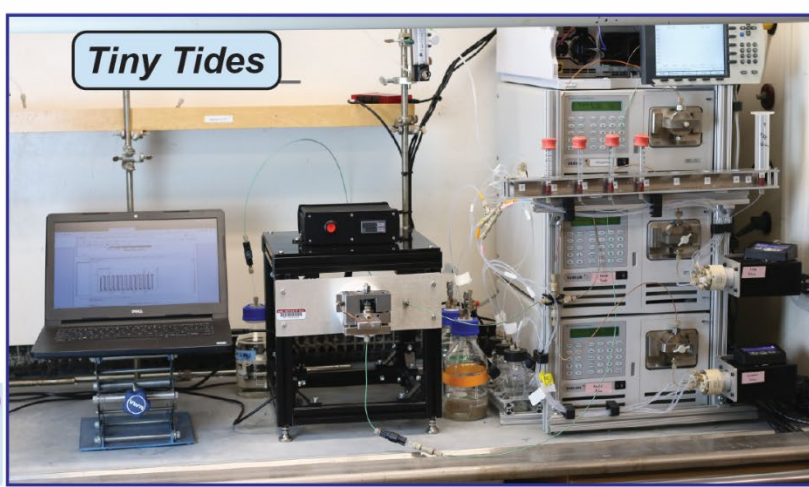
Figure 1. *Automated flow synthesis of PMOs at 90 °C provides rapid access to new therapeutic candidates.*
a) Dystrophin is an integral membrane protein that anchors the cytoskeleton to the muscle cell membrane
via the dystrophin associated muscle complex (DAPC). Little to no natural dystrophin is produced in patients
with Duchenne muscular dystrophy (DMD). The PMO Vyondys 53™ induces skipping of exon 53 to regain
the proper reading frame, producing shorter but functional dystrophin. b) Vyondys 53™ is a 25-mer fully
synthetic antisense phosphorodiamidate morpholino oligomer. PMOs are the only available treatment for
DMD, but the two currently approved drugs combined can only treat 25% of DMD patients. Given that 80%
of patients have DMD subtypes that are amenable to exon skipping treatments, more work remains to be
done. c) Development of PMO drugs requires testing of many sequences and laborious production of
sequential revisions. An automated fast-flow synthesizer allows for rapid manufacture of PMO sequences
at 90 °C.

Results

Increasing the temperature of PMO synthesis significantly decreases reaction times, contingent on the stability of reagents. PMOs are synthesized from the 5'- to the 3'-end on a crosslinked polystyrene solid support[1, 26, 31, 32] (Fig. 2a). Nucleotides are incorporated using 3'-triphenylmethyl (trityl) protected phosphoramido chloridate monomers with a tertiary amine base in solution. Trityl protection is removed in acid to regenerate, after a neutralization step, a reactive 3'-amine for the next coupling. Monomer coupling dominates the synthesis time, and was the major focus for optimization of our methodology.

Temperatures of over 70 °C will accelerate both on target and off-target reactions, with degradation of synthetic intermediates limiting the maximum possible synthesis temperature. To determine the maximum reaction temperature, we tracked degradation of the phosphoramido chloridate monomers and the resin bound PMO in synthetic conditions at various temperatures.

Monomer Stability Study.

The thermal stability of the activated phosphoramido chloridate monomers used for coupling, determined 90 °C as the maximum temperature for flow synthesis. While not necessary for room temperature procedures, anhydrous conditions are required at 90 °C. Of particular interest was the propensity for the monomers to decompose via polymerization.

To determine the maximum allowed temperature for a flow synthesis, we assayed the thermally induced degradation of each monomer (moA, moT, moC, moG) at gradually increasing temperature. In sealed vials, 0.2 M coupling solutions of activated, protected morpholino monomer and 0.4 M *N,N*-diisopropylethylamine (DIEA) in 1,3-dimethyl-2-imidazolidinone (DMI) were heated for 5 minutes at temperatures from 90 °C to 150 °C (Fig. 2b). After 5 minutes, coupling solutions were quenched with a 10% (v/v) solution of piperidine in *N*-methyl-2-pyrrolidone (NMP) and analyzed by liquid chromatography-mass spectrometry (LC-MS). Degradation was characterized by the disappearance of the major peak of the piperidine-quenched monomers and the increase in uncharacterized side-

139 product peaks. Stability was evaluated over 5 minutes because this was the predicted
140 residence time following rapid preheating in a flow system.

141 All activated monomers ware stable at temperatures up to 90 °C, setting this as a
142 conservative upper temperature limit (see Supplementary Fig. 6). The moA monomer
143 degraded to unknown products at higher temperatures (Fig. 2b).

Resin-Bound PMO Stability Study

145 Protected PMO attached to a solid support does not degrade at 90 °C in the
146 solvents used for room temperature syntheses. Although we were unable to find any
147 reports of instability of the resin-bound protected PMO chain in the standard wash
148 solvents, dichloromethane (DCM), DMI, and neutralization solution made from 5% 4-
149 ethylmorpholine (NEM) in 3:1 DCM to isopropanol (v/v), we investigated this behavior at
150 90 °C. A protected resin-bound PMO with the sequence 5'-CTCCAACATC-3' was treated
151 with these solvents at elevated temperatures for 4 hours. For most conditions tested,
152 90 °C was chosen to emulate the maximum possible temperature from the monomer
153 studies. The only exception to this was DCM which was performed at 70 °C. The lower
154 temperature was chosen to reduce pressure in the glass vials used. The 4-hour treatment
155 time was selected since it is an excess of the time required for a typical flow synthesis.
156 The resin was isolated, washed, cleaved, and degradation was measured using LC-MS.
157 Thermal degradation of PMOs produce a complex mixture of side products that often co-
158 elute in LC-MS separations. We observed that significant degradation occurred in non-
159 standard synthesis solvents (see Supplementary Fig. 8). When the PMO chain was
160 treated with DCM, DMI, or neutralization solution, however, no degradation products were
161 observed (Fig. 2c).

Detritylation Optimization at 90 °C.

163 The protected PMO chain is known to be unstable to acidic conditions[26], so use of
164 a milder acid is required for 90 °C detritylation. Although use of typical acid mixtures at
165 90 °C removes the 3'-trityl group rapidly, it also severely degrades the PMO chain on the
166 same time scale (see Supplementary Fig. 9). Room temperature PMO syntheses use the
167 conjugate acid of substituted heterocycles to fine-tune acid strength[26], and we reasoned

168   that the same strategy can be applied to find a reagent for use at 90 °C. Of special interest

169   was the substituted pyridine class of reagents, and among these 4-cyanopyridine

170   trifluoroacetate is the most effective in room temperature syntheses[26].

171   A series of less acidic substituted pyridine trifluoroacetates were tested, and 3,5-

172   lutidine was found to lead to rapid deprotection but slow degradation (Fig. 2d). A protected,

173   resin-bound 4-mer PMO with the sequence 5'-ACGT-Trityl-3' was treated with

174   trifluoroacetate salts of 4-cyanopyridine (control, pK_a = 1.9)[33], pyridine (pK_a = 5.2)[34], 3,5-

175   lutidine (pK_a = 6.1)[35], and 2,4,6-collidine (pK_a = 7.5)[34] at room temperature or 90 °C.

176   Reagent solutions include 100 mM of each pyridine trifluoroacetate in 30%

177   trifluoroethanol (TFE), 69% DCM and 1% ethanol (v/v/v). Time points were taken at 1, 30,

178   and 120 minutes and analyzed by LC-MS. Treatment at 120 minutes is representative of

179   the cumulative deprotection time after a full synthesis. All reagents except collidine

180   trifluoroacetate were able to completely remove the trityl group in one minute as tracked

181   by the loss of trityl-on peak at 15.5 minutes in the LC-MS trace. Pyridine and

182   cyanopyridine trifluoroacetates were too acidic and lead to degradation of the PMO chains

183   through deamidation of the phosphorodiamidate linkages presenting at 11.9 minutes in

184   the LC-MS trace. 3,5-Lutidine was chosen for further studies as it avoided degradation at

185   the longest treatment time, but also led to full deprotection in under one minute.
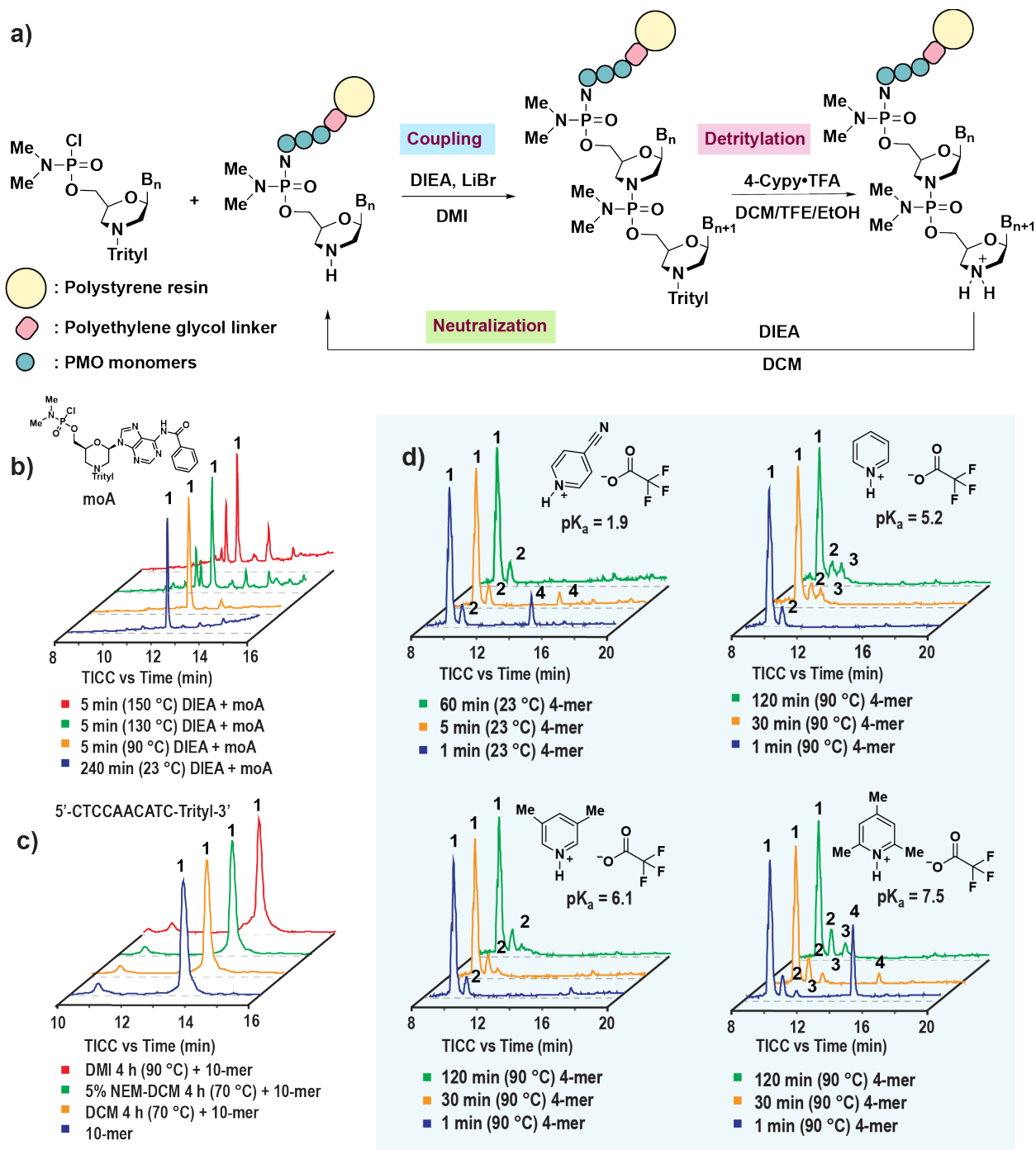
Figure 2. PMO synthetic conditions can be adapted to 90 °C. a) Each nucleotide is incorporated as a trityl-protected phosphoramido chloridate in DMI. Detritylation frees the 3'-terminal amine with the conjugate acid of a non-nucleophilic heterocycle, typically 4-cyanopyridine in dichloromethane-trifluoroethanol mixtures. Neutralization of the 3'-amine prepares the chain for the next coupling reaction using tertiary amine bases in DCM/isopropanol mixtures. b) The activated PMO monomer for the nucleobase adenine is stable for 5 minutes at 90 °C. Higher temperatures lead to degradation of the activated monomer species. Peak 1 in

193　*the LCMS trace represents the remaining active monomer, and as temperature is increased, peak 1*
194　*diminishes compared to degradation products. c) Resin-bound 10-mer PMO is stable to 90 °C incubation*
195　*for 4 hours in wash solvents. d) The 3'-triphenylmethyl group (Trityl) of the 4-mer PMO sequence 5'-ACGT-*
196　*Trityl-3' is quantitatively removed in 10 minutes by both 4-cyanopyridine trifluoroacetate at room*
197　*temperature and 3,5-lutidine at 90 °C. Trityl group loss is monitored by disappearance of peak 4, and*
198　*degradation is tracked by increases in peak 3. Peaks 1 and 2 represent resolved diastereomers of the intact*
199　*deprotected PMO chain.*

200　**Design of an Automated Microscale Flow Synthesizer**.

201　　　A microscale instrument to carry out the flow synthesis of PMOs was constructed
202　from commercially available components and a machined reaction vessel using a design
203　similar to a previously reported fast-flow peptide synthesizer[36]. The base design consists
204　of 6 modules connected in series (Fig. 3a). The first module is a collection of glass
205　containers with liquid reagents stored under nitrogen. Two chemically inert valves
206　compose the second module. Under computer control, each valve chooses its input from
207　the available reagents in module one, updating throughout a run. The third module is
208　composed of two HPLC pumps, each connected to one of the outputs from module 2.
209　Each pump is capable of　supplying up to 2.5 mL per minute limited by reagent viscosity
210　and pump configuration. The output streams from module 3 meet in a T-mixer and then
211　travel to module 4, the reaction vessel module. Flow enters module 4 and is passed
212　through a 90 cm long metal tube over a heated aluminum core bringing the solution to
213　temperature in about 2 seconds. Module 4 holds the solid-phase resin in a removable
214　reactor chamber 1 mL in volume at the desired temperature. The pre-heated flow passes
215　through the resin, reacting with the growing PMO chains. Module 5 is a UV-Vis detector
216　used to monitor the composition of the spent reagent solution in-line. Module 6 is a
217　computer that controls all other modules using a modular script in the Mechwolf
218　programming environment[37].
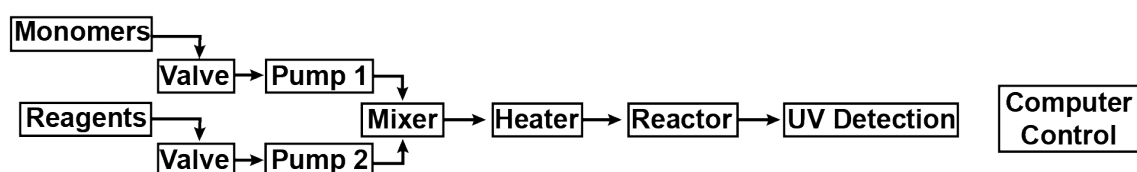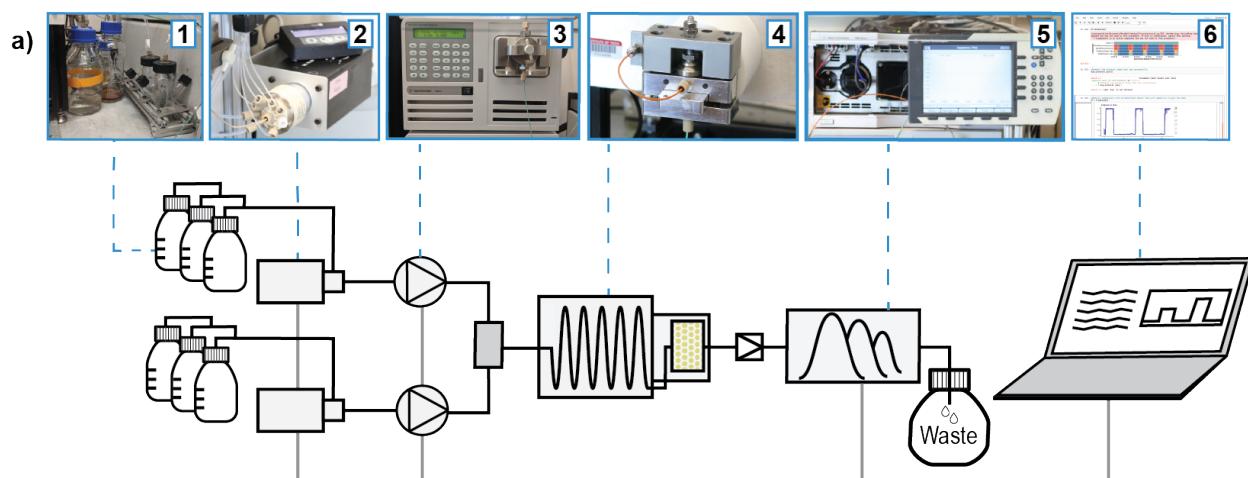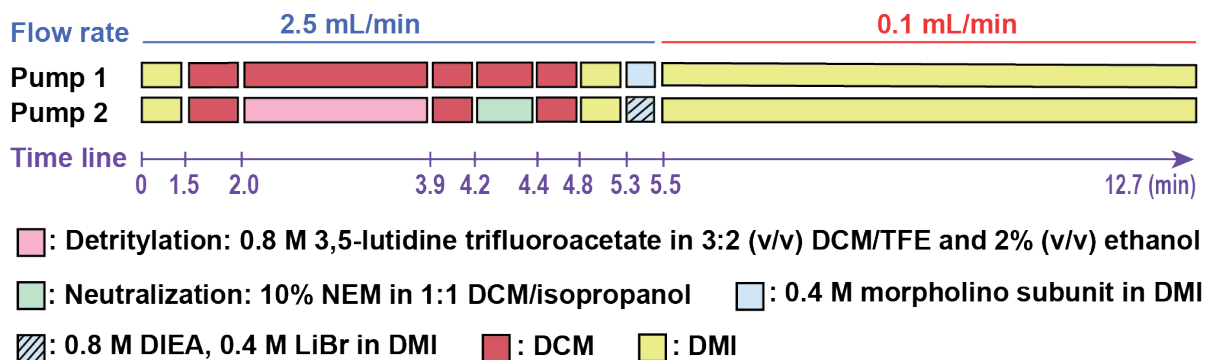
Figure 3. The reported automated fast-flow instrument features 6 modules that act to effect rapid PMO synthesis. a) A schematic for the flow-path of the instrument is shown. Valves select the appropriate solutions from glass bottles under nitrogen pressure. Two HPLC pumps mix the reagents and flow them over a packed resin bed held at 90 °C. Effluent cools as it exits the reactor and passes through a back-pressure regulator to an in-line UV-Vis detector where reaction progress is monitored. A computer running an automated Python script controls the valves and pumps throughout the synthesis and tracks the instrument performance from the UV-Vis detector. b) The optimized protocol for PMO synthesis is shown. Instructions are delivered by the control program to the pumps and valves at each of the listed times. Bars represent activity of the two HPLC pumps, and colors indicate which reagents the valves are open to. Reagent stocks are prepared in double the concentration that is intended to hit the resin. Dilution from the second pump prepares the correct concentrations upon mixing.

231   This design allows for precise control of reaction conditions for microscale PMO
232   synthesis. The reactor body is designed for a 4.4 μmol-scale synthesis, the equivalent of
233   10 mg of a medium loading resin (0.39-0.43 mmol/g). Reagent delivery is encoded using
234   pump strokes and flow rate. Each stroke of the HPLC pump carries 40 μL of solvent and
235   it takes 12 strokes from both pumps (960 μL) to reach the resin. Flow rate is adjusted by
236   increasing both the time to deliver strokes, and the time between strokes. Reaction time
237   on the resin can be increased by increasing the number of pump strokes, or by decreasing
238   the flow rate once the reagents hit the resin. Clearance of regents from the reservoir takes
239   20 pump strokes (1.6 mL), so reaction steps are separated by washes of at least 20
240   strokes of the appropriate wash solvent.

241   The optimized synthesis sequence with controls for each module can be seen in
242   Fig. 3b. A discussion about optimization of individual parts of the instrument is provided
243   in the Supplementary Section 10.

244   **Optimization of Automated Fast-Flow Synthesis**

245   Iterative changes in flow synthesis variables were used to develop a flow recipe
246   that can produce PMO sequences of similar purity during room temperature syntheses.
247   Solid-phase PMO synthesis is sensitive to small variations in reaction efficiency, as the
248   many reactions in series amplify off-target pathways. We took advantage of this
249   amplification to optimize reactions in flow. For each variable of interest, we synthesized
250   a 4-mer PMO, a process that involves 12 sequential reaction steps. Using LC-MS, we
251   compared the crude purity of the products from each reaction sequence. Timings and
252   reagents for each synthesis were as shown in Fig. 3b with the modifications listed in Fig.
253   4. The actions that the Python script sends to modules 2 and 3 throughout the synthesis
254   cycle are shown in Fig. 3. The resulting resin-bound PMO product was cleaved, the
255   sample analyzed by LC-MS, and the relative levels of the product and high molecular
256   weight side-products were quantified using a molecular feature extraction utility. Of
257   special interest were side-products arising from incomplete couplings, and we tracked
258   their relative abundance separately.

259   Use of the highest allowable temperature determined from monomer and resin-
260   bound PMO stability studies, 90 °C, provided the cleanest crude PMO. Initial reaction
261   screens were carried out at 70 °C, a milder temperature that enables use of the standard
262   4-cyanopyridine trifluoroacetate deprotection solution without the significant degradation
263   found at 90 °C (see Supplementary Fig. 9). Initial results from flow synthesis at 70 °C
264   provided the desired material but with a crude purity of 72%, lower than the benchmark
265   95% from room temperature syntheses (Fig. 4 entries 1 vs 2). Further optimization with
266   changes to the instrument command recipe, monomer equivalents, and coupling catalysts
267   improved crude purity to 92% (Fig. 4 entries 3 to 6). Detectable levels of side-products
268   remained, so improvement of the coupling reaction was still required. Although increasing
269   monomer excess would likely increase crude purity, we capped this value at 18
270   equivalents, a generally accepted upper limit in academic and patent literature[10, 26]. We
271   instead increased the temperature to 90 °C to improve coupling rates. Along with
272   optimization of deprotection conditions, neutralization and coupling bases (Fig. 4 entries
273   7 to 10), the increase in temperature provided an optimized recipe that yields a crude
274   purity of 99% (Fig. 4 entry 11). This protocol was used for the production of the sequences
275   reported in the remainder of this work.

276   The final experiment shown in Fig. 4 (entry 12) demonstrates that high temperature
277   flow synthesis of PMOs does not require more monomer equivalents than room
278   temperature protocols. The phosphoramido chloridate monomers are costly, and it is
279   common to minimize the excess used. Using the standard 10 equivalents at high
280   temperature is effective, but requires a longer coupling step with this hardware
281   configuration.

|	Detritylation	Neutralization	Coupling				Instrument			Side Products				
Entry	Deprotection Reagent	Neutralization Reagent	Coupling Base	Additive	Monomer Equivalents	Coupling Time (min)	Temperature (°C)	Crude Purity	A Deletion (%)	T Deletion (%)	C Deletion (%)	G Deletion (%)	Uncharacterized (%)
1	4-Cypy•TFA	DIEA	DIEA	none	10	143	r.t.	**95%**	n.d.	n.d.	n.d.	n.d.	5.0
2	4-Cypy•TFA	DIEA	DIEA	none	10	17.4	70	**72%**	0.6	5.7	n.d.	9.9	11.8
3	4-Cypy•TFA	DIEA	DIEA	none	10	11.7	70	**74%**	0.7	5.6	0.3	11.3	8.1
4	4-Cypy•TFA	DIEA	DIEA	none	18	11.7	70	**85%**	n.d.	1.9	n.d.	3.6	9.5
5	4-Cypy•TFA	DIEA	DIEA	NMI	18	11.7	70	**87%**	n.d.	1.1	n.d.	1.3	10.6
6	4-Cypy•TFA	DIEA	DIEA	LiBr	18	11.7	70	**92%**	n.d.	0.9	n.d.	2.6	4.5
7	4-Cypy•TFA	DIEA	DIEA	LiBr	18	11.7	90	**82%**	n.d.	n.d.	n.d.	1.8	16.2
8	3,5-Lut•TFA	DIEA	DIEA	LiBr	18	12.6	90	**93%**	n.d.	n.d.	n.d.	1.5	5.5
9	3,5-Lut•TFA	DIEA	NEM	LiBr	18	12.6	90	**92%**	n.d.	n.d.	n.d.	1.5	6.5
10	3,5-Lut•TFA	NEM	DIEA	LiBr	18	12.6	90	**95%**	n.d.	n.d.	n.d.	1.3	3.7
11*	3,5-Lut•TFA	NEM	DIEA	LiBr	18	12.7	90	**99%**	n.d.	n.d.	n.d.	0.9	0.1
12*	3,5-Lut•TFA	NEM	DIEA	LiBr	10	22.1	90	**96%**	n.d.	n.d.	n.d.	1.5	2.5

Figure 4. Optimized flow synthesis produces PMOs with similar purity to manual batch protocols. Synthesis variables were changed in sequence, and relative crude purities were tracked by comparison of the crude LC-MS traces. Crude purity was quantified by analysis of the total ion current chromatograms (TICCs). All ions from the same parent compound were summed, and the ion counts between compounds compared. Crude purity is reported as the percentage of the total ion current at the molecular weight of the 4-mer PMO sequence. Deletion sequences arising from incomplete couplings were quantified using the same method. Additional details are included in the Supplementary Section 6. *The Python script was edited to slowly deliver the monomers, reducing flow inaccuracies due to the viscous solution of the G monomer N.d. = levels were below the sensitivity of detection with the described quantification method – not detected.

The Microscale Flow Synthesizer Rapidly Produces Potential Therapeutic PMO Sequences.

The optimized high temperature flow recipe provides PMO sequences with similar purity to room temperature protocols in a fraction of the time. Synthesis of an 18-mer PMO, which hybridizes to the β-thalassemia gene sequence, IVS2-654[38, 39] using batch protocols takes 1 full week. The flow protocol enables the production of the full PMO sequence in only 3.5 hours. The crude products were of comparable purity by LC-MS (Fig.

299 5a and c). 20 mg of each sample were purified, to afford 1 mg of material more than 85%
300 pure (Fig. 5b and d).

301
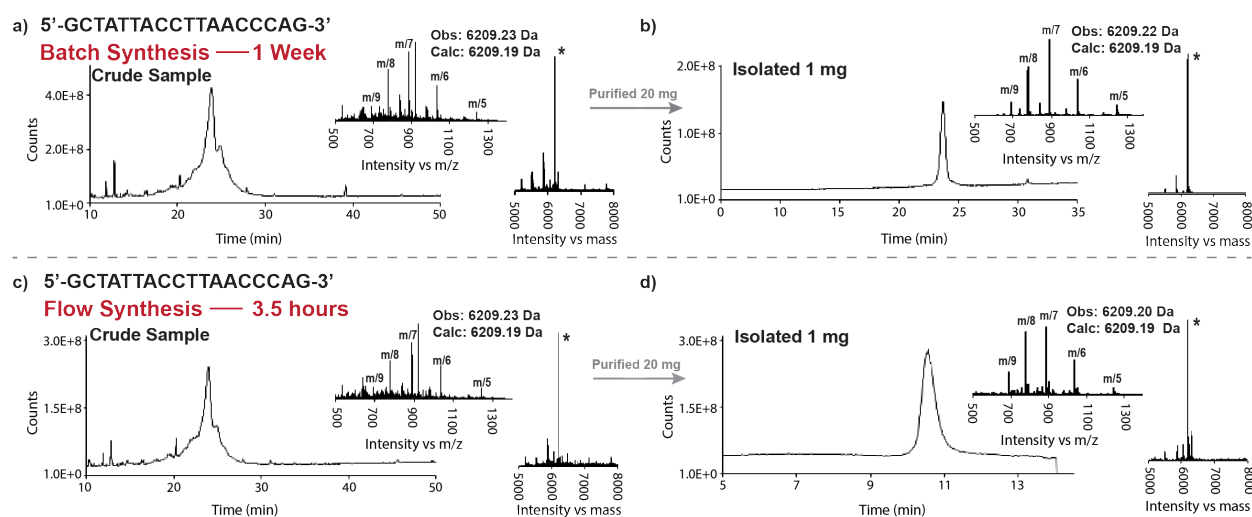
Figure 5. *Fast-flow and batch syntheses of an 18-mer PMO deliver crude products with similar purity. a)*
The TICC of a batch-synthesized sample of the 18-mer PMO IVS2-654 is shown along with the mass
spectrum and associated deconvoluted mass spectrum. b) The TICC of the batch-synthesized sample after
purification by cation exchange chromatography is shown along with the mass spectrum and associated
deconvoluted mass spectrum. c) The TICC, mass spectrum and deconvoluted mass spectrum are shown
for the crude product from a flow synthesis of the same 18-mer sequence. d) The TICC of the flow-
synthesized sample after purification along with the mass spectrum and deconvoluted mass spectrum. Note:
Traces B and D were acquired using different LC-MS methods.

310 After demonstrating the efficacy of fast-flow synthesis of PMO, we leveraged the
311 platform for rapid production of new potential therapeutics. We synthesized three PMO
312 sequences targeted to skip exon 46 of *DMD* pre-mRNA. Although exon skipping at this
313 site has an important place in the history of splice alteration for *DMD*[40], no treatment
314 options are available that target exon 46. Three sequences near splice acceptor and
315 donor sites were chosen as previously reported[41] (Fig. 6a). Using the automated fast-flow
316 instrument, the three 20-mer sequences were synthesized in a single day in succession.
317 In each case, after cleavage and purification, 1 mg of PMO material was isolated with
318 greater than 85% purity. Manufacturing these three sequences under batch conditions
319 would take approximately one month if done sequentially (Fig. 6b).

15

320   Further, PMOs used as steric block antisense compounds provide a potential route
321   to inhibit viral replication. We designed and synthesized a PMO sequence to inhibit
322   SARS-CoV-2 replication in only 3.5 hours. Using room temperature synthesis,
323   manufacturing each new potential COVID-19 therapeutic would take at least a week. The
324   18-mer PMO was targeted to the transcription regulatory sequence (TRS) stem loop of
325   the 5'UTR of the genomic mRNA (Fig. 6c), a strategy that proved effective for treatment
326   of the closely related SARS-CoV[29]. Purification of 12 mg of the crude sample (one third
327   of total) afforded 0.3 mg of PMO with >90% purity (Fig. 6d).
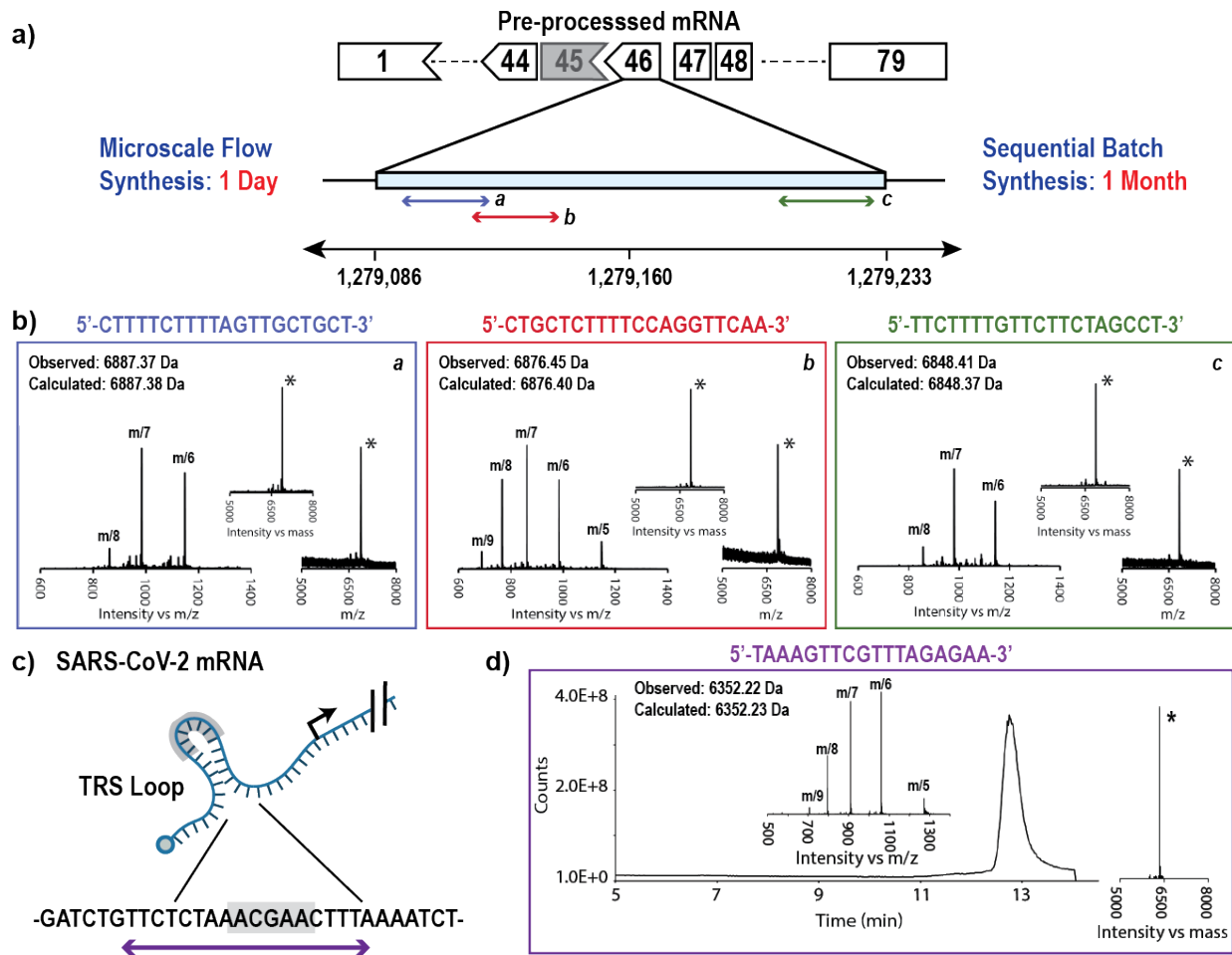
328

329   **Figure 6**. *Automated flow synthesis enables the rapid production of therapeutic candidates for diverse*
330   *diseases. a) Gene diagram showing the splicing sites where the three potential therapeutic sequences are*
331   *targeted. Three sequences were chosen for targeting splice donor and acceptor sites of exon 46. b) The*
332   *mass spectrum, deconvoluted mass spectrum and MALDI mass spectra of purified PMOs synthesized in*
333   *flow is shown (see Supplementary Section 13.4). c) The 5' UTR TRS is conserved between coronaviruses,*
334   *and is a target for antisense knockdown of viral replication. The TRS is shown in grey, and a sequence was*

16

Discussion

339   The fast-flow synthesizer developed here enables rapid pre-heating of reagents
340   and efficient heat and mass transfer within the resin bed on a scalable, mechanically
341   robust platform. With these features, we adapted PMO synthesis to 90 °C and ultimately
342   succeeded in decreasing coupling time from three hours per nucleotide to 8 minutes.
343   Further, this microscale platform successfully balances production of sufficient PMO for
344   biological testing while conserving costly PMO monomers.

345   Fast flow synthesis will be a valuable tool in capitalizing on the recent successes
346   of PMO antisense treatments[2, 3] to expand PMOs to treat new diseases. With rapid flow
347   synthesis, the production of novel PMO therapeutics will be freed from long lead
348   optimization cycles. To demonstrate the power of this flow platform, we synthesized three
349   candidates for a new DMD treatment in a single day, and we anticipate that the
350   development of new PMO drugs using this platform will be similarly accelerated. Given
351   the urgent circumstances around the global COVID-19 pandemic, such timeline
352   reductions are urgently needed, and we demonstrated here the utility of fast PMO
353   synthesis by producing a potential antisense antiviral treatment in only 3.5 hours.

354   Overall, our results illustrate that machine control of flow chemistry can improve
355   synthetic outcomes beyond what is possible with manual techniques. The strategy in this
356   work is applicable to diverse polymer backbones, and we envision high temperature
357   automated flow synthesis will enable development of new on-demand biopolymers that
358   may currently be inaccessible due to tedious, difficult, or impractical syntheses.

Methods

360   The following procedure was used for automated flow synthesis. Aminomethyl
361   polystyrene resin loaded with a PEG_3 tail (see Supplementary Section 3.1) (10 mg, 0.39-
362   0.43 mmol/g loading) was loaded into the reactor, the reactor was connected to the
363   reactor head and heated to 90 °C. DCM was delivered at 5 mL/min (2.5 mL/min per pump)

17

364 for 30 seconds to remove air. The flow was stopped and the resin was allowed to swell

365 at 90 °C for 5 minutes. The flow protocol was started with an initial DMI wash at 5 mL/min

366 (2.5 mL/min per pump) for 90 seconds, then a DCM wash at 5 mL/min (2.5 mL/min per

367 pump) for 30 seconds. Detritylation was performed with one-part 800 mM 3,5-lutidine

368 trifluoroacetate in 3:2 (v/v) DCM/TFE + 2% (v/v) ethanol, and one-part DCM for 114

369 seconds at the same flow rate. After an 18-second DCM wash, neutralization was

370 performed with one-part 10% NEM in 1:1 DCM/isopropanol and one-part DCM for 12

371 seconds. The resin was then washed with DCM for 24 seconds, and DMI for 30 seconds,

372 each at 5 mL/min (2.5 mL/min per pump). Coupling solution composed of one-part 0.4 M

373 morpholino subunit in DMI and one-part 0.8 M DIEA with 0.4 M LiBr in DMI was delivered

374 at 5 mL/min (2.5 mL/min per pump) for 12 seconds (0.079 mmol monomer). DMI was

375 delivered at 5 mL/min (2.5 mL/min per pump) until the monomer solution arrived at the

376 reactor (12 strokes total). DMI was delivered at 0.1 mL/min for 432 seconds. This protocol

377 was repeated for each residue until synthesis was complete. A final deprotection was

378 carried out with the same detritylation reagent and conditions. The resin was removed

379 from the reactor, washed 5 times with DCM in a fritted syringe (Torviq), dried under

380 vacuum, and cleaved (See Supplementary Information, Section 4 method 2). The crude

381 products were captured on a polystyrene reverse phase resin, and eluted with 50%

382 aqueous acetonitrile into a pre-weighed 10 mL conical centrifuge tube. The sample was

383 lyophilized to afford the crude PMO as a white powder suitable for LC-MS analysis and

384 preparative cation exchange purification.

385 **Code availability**

386   The Python code for automated operation of the flow synthesis instrument is

387 available in a GitHub repository (http://doi.org/10.5281/zenodo.3774509).

388 **Data availability**

389   All the data generated or analyzed during this study are included in this published

390 article (and in the Supplementary Information). Further details are available from the

391 corresponding authors upon request.

392

References

1. Summerton, J. & Weller, D. Morpholino antisense oligomers: design, preparation, and properties. *Antisense Nucleic Acid Drug Dev.* **7**, 187-195 (1997).

2. Heo, Y.-A. Golodirsen: first approval. *Drugs* **80**, 329-333 (2020).

3. Syed, Y. Y. Eteplirsen: first global approval. *Drugs* **76**, 1699-1704 (2016).

4. van Deutekom, J. C. & van Ommen, G. J. Advances in Duchenne muscular dystrophy gene therapy. *Nat. Rev. Genet.* **4**, 774-783 (2003).

5. Holden, K. L., Stein, D. A., Pierson, T. C., Ahmed, A. A., Clyde, K., Iversen, P. L. & Harris, E. Inhibition of dengue virus translation and RNA synthesis by a morpholino oligomer targeted to the top of the terminal 3′ stem–loop structure. *Virology* **344**, 439-452 (2006).

6. Iversen, P. L., Warren, T. K., Wells, J. B., Garza, N. L., Mourich, D. V., Welch, L. S., Panchal, R. G. & Bavari, S. Discovery and early development of AVI-7537 and AVI-7288 for the treatment of Ebola virus and Marburg virus infections. *Viruses* **4**, 2806-2830 (2012).

7. Ge, Q., Pastey, M., Kobasa, D., Puthavathana, P., Lupfer, C., Bestwick, R. K., Iversen, P. L., Chen, J. & Stein, D. A. Inhibition of multiple subtypes of influenza a virus in cell cultures with morpholino oligomers. *Antimicrob. Agents Chemother.* **50**, 3724-3733 (2006).

8. Hudziak, R. M., Barofsky, E., Barofsky, D. F., Weller, D. L., Huang, S.-B. & Weller, D. D. Resistance of morpholino phosphorodiamidate oligomers to enzymatic degradation. *Antisense Nucleic Acid Drug Dev.* **6**, 267-272 (1996).

9. Arora, V., Knapp, D. C., Reddy, M. T., Weller, D. D. & Iversen, P. L. Bioavailability and efficacy of antisense morpholino oligomers targeted to c-myc and cytochrome P-450 3A2 following oral administration in rats. *J. Pharm. Sci.* **91**, 1009-1018 (2002).

419   10. Bhadra, J., Pattanayak, S. & Sinha, S. Synthesis of morpholino monomers,
420   chlorophosphoramidate monomers, and solid-phase synthesis of short
421   morpholino oligomers. *Curr. Protoc. Nucleic Acid Chem.* **62**, 4.65.1-4.65.26
422   (2015).

423   11. Caruthers, M. H. Gene synthesis machines: DNA chemistry and its uses. *Science*
424   **230**, 281-285 (1985).

425   12. Behrendt, R., White, P. & Offer, J. Advances in Fmoc solid-phase peptide
426   synthesis. *J. Pept. Sci.* **22**, 4-27 (2016).

427   13. Hartrampf, N., Saebi, A., Poskus, M., Gates, Z. P., Callahan, A. J., Cowfer, A. E.,
428   Hanna, S., Antilla, S., Schissel, C. K., Quartararo, A. J., Ye, X., Mijalis, A. J.,
429   Simon, M. D., Loas, A., Liu, S., Jessen, C., Nielsen, T. E. & Pentelute, B. L.
430   Synthesis of proteins by automated flow chemistry. *Science* **368**, 980-987 (2020).

431   14. Beaucage, S. L. & Caruthers, M. H. Deoxynucleoside phosphoramidites—A new
432   class of key intermediates for deoxypolynucleotide synthesis. *Tetrahedron Lett.*
433   **22**, 1859-1862 (1981).

434   15. Dawson, P., Muir, T., Clark-Lewis, I. & Kent, S. Synthesis of proteins by native
435   chemical ligation. *Science* **266**, 776-779 (1994).

436   16. Rodriguez-Garcia, M., Surman, A. J., Cooper, G. J. T., Suárez-Marina, I., Hosni,
437   Z., Lee, M. P. & Cronin, L. Formation of oligopeptides in high yield under simple
438   programmable conditions. *Nat. Commun.* **6**, 8385 (2015).

439   17. McQuade, D. T. & Seeberger, P. H. Applying flow chemistry: methods, materials,
440   and multistep synthesis. *J. Org. Chem.* **78**, 6384-6389 (2013).

441   18. Hartman, R. L., McMullen, J. P. & Jensen, K. F. Deciding whether to go with the
442   flow: evaluating the merits of flow reactors for synthesis. *Angew. Chem. Int. Ed.*
443   **50**, 7502-7519 (2011).

444   19. Kobayashi, S. Flow "fine" synthesis: high yielding and selective organic synthesis
445   by flow methods. *Chem. Asian J.* **11**, 425-436 (2016).

446 20. Ley, S. V., Fitzpatrick, D. E., Ingham, Richard. J. & Myers, R. M. Organic
447   synthesis: march of the machines. *Angew. Chem. Int. Ed.* **54**, 3449–3464 (2015).

448 21. Schnölzer, M., Alewood, P., Jones, A., Alewood, D. & Kent, S. B. H. In situ
449   neutralization in boc-chemistry solid phase peptide synthesis. *Int. J. Pept. Res.*
450   *Ther.* **13**, 31-44 (2007).

451 22. Plante, O. J., Palmacci, E. R. & Seeberger, P. H. Automated solid-phase
452   synthesis of oligosaccharides. *Science* **291**, 1523-1527 (2001).

453 23. Yoshida, J.-i., Takahashi, Y. & Nagaki, A. Flash chemistry: flow chemistry that
454   cannot be done in batch. *Chem. Commun.* **49**, 9896-9904 (2013).

455 24. Truex, N. L., Holden, R. L., Wang, B.-Y., Chen, P.-G., Hanna, S., Hu, Z., Shetty,
456   K., Olive, O., Neuberg, D., Hacohen, N., Keskin, D. B., Ott, P. A., Wu, C. J. &
457   Pentelute, B. L. Automated flow synthesis of tumor neoantigen peptides for
458   personalized immunotherapy. *Scientific Reports* **10**, 723 (2020).

459 25. Jiang, T., Bordi, S., McMillan, A. E., Chen, K. -Y., Saito, F., Nichols, P., Wanner,
460   B. & Bode, J. An integrated console for capsule-based, fully automated organic
461   synthesis. Preprint at doi:10.26434/chemrxiv.7882799.v1. (2019).

462 26. Fox, C. M. J. & Weller, D. D. Method of synthesis of morpholino oligomers. US
463   patent 8299206 B2 (2008).

464 27. Dong, E., Du, H. & Gardner, L. An interactive web-based dashboard to track
465   COVID-19 in real time. *Lancet Infect Dis.* **20**, 533-534 (2020).

466 28. Liu, C., Zhou, Q., Li, Y., Garner, L. V., Watkins, S. P., Carter, L. J., Smoot, J.,
467   Gregg, A. C., Daniels, A. D., Jervey, S. & Albaiu, D. Research and development
468   on therapeutic agents and vaccines for COVID-19 and related human
469   coronavirus diseases. *ACS Cent. Sci.* **6**, 315-331 (2020).

470 29. Neuman, B. W., Stein, D. A., Kroeker, A. D., Churchill, M. J., Kim, A. M., Kuhn,
471   P., Dawson, P., Moulton, H. M., Bestwick, R. K., Iversen, P. L. & Buchmeier, M.
472   J. Inhibition, escape, and attenuated growth of severe acute respiratory

473   syndrome coronavirus treated with antisense morpholino oligomers. *J. Virol.* **79**,
474   9665-9676 (2005).

475   30. Burrer, R., Neuman, B. W., Ting, J. P. C., Stein, D. A., Moulton, H. M., Iversen,
476   P. L., Kuhn, P. & Buchmeier, M. J. Antiviral effects of antisense morpholino
477   oligomers in murine coronavirus infection models. *J. Virol.* **81**, 5637-5648 (2007).

478   31. Summerton, J. E. & Weller, D. D. Uncharged morpholino-based polymers having
479   phosphorous containing chiral intersubunit linkages. US patent 5185444 (1991).

480   32. Harakawa, T., Tsunoda, H., Ohkubo, A., Seio, K. & Sekine, M. Development of
481   an efficient method for phosphorodiamidate bond formation by using inorganic
482   salts. *Bioorg. Med. Chem. Lett.* **22**, 1445-1447 (2012).

483   33. Porter, R. S. & Johnson, J. F. *Analytical Calorimetry: Proceedings of the*
484   *Symposium on Analytical Calorimetry at the meeting of the American Chemical*
485   *Society* (Springer, 1970).

486   34. Grandberg, I. I., Faizova, G. K. & Kost, A. N. Comparative basicities of
487   substituted pyridines and electronegativity series for substituents in the pyridine
488   series. *Chem. Heterocycl. Compd.* **2**, 421-425 (1967).

489   35. Clarke, K. & Rothwell, K. A kinetic study of the effect of substituents on the rate
490   of formation of alkylpyridinium halides in nitromethane solution. *J. Chem. Soc.* **0**
491   1885-1895 (1960).

492   36. Simon, M. D., Heider, P. L., Adamo, A., Vinogradov, A. A., Mong, S. K., Li, X.,
493   Berger, T., Policarpo, R. L., Zhang, C., Zou, Y., Liao, X., Spokoyny, A. M., Jensen,
494   K. F. & Pentelute, B. L. Rapid flow-based peptide synthesis. *ChemBioChem* **15**,
495   713-720 (2014).

496   37. Benjamin Lee, amijalis, littleblackfish & NLPohl. a-callahan/MechWolf_Pull 0.1.1.
497   (2020). doi:10.5281/zenodo.3774509.

498   38. Wolfe, J. M., Fadzen, C. M., Holden, R. L., Yao, M., Hanson, G. J. & Pentelute,
499   B. L. Perfluoroaryl bicyclic cell-penetrating peptides for delivery of antisense
500   oligonucleotides. *Angew. Chem. Int. Ed.* **57**, 4756-4759 (2018).

39. Sazani, P., Kang, S.-H., Maier, M. A., Wei, C., Dillman, J., Summerton, J., Manoharan, M. & Kole, R. Nuclear antisense effects of neutral, anionic and cationic oligonucleotide analogs. *Nucleic Acids Res.* **29**, 3965-3974 (2001).

40. van Deutekom, J. C. T., Bremmer-Bout, M., Janson, A. A. M., Ginjaar, I. B., Baas, F., den Dunnen, J. T. & van Ommen, G.-J. B. Antisense-induced exon skipping restores dystrophin expression in DMD patient derived muscle cells. *Hum. Mol. Genet.* **10**, 1547-1554 (2001).

41. Sazani, P. & Kole, R. Multiple exon skipping compositions for DMD. US patent 9434948 B2 (2015).

Acknowledgements

Author contributions

C.L. and A.J.C. built the updated PMO synthesizer, improved the Python program, optimized fast-flow synthesis conditions, synthesized and purified PMO IVS2-654, three 20-mer PMO drug candidates, and the SARS-CoV-2 drug candidate. M.D.S. and K.A.T. performed PMO stability studies. A.J.M. and N.L.B.P. designed the open source synthesis software, Mechwolf. A.J.M. helped build the PMO synthesizer. N.H. and C.K.S. helped update the PMO synthesizer. M.Z., H.Z. and G.K.H. provided input on optimization of the PMO synthesis cycle. C.L., A.J.C., M.J.S, K.A.T, and B.L.P. conceptualized the research and designed the experiments. C.L., A.J.C., A.L., M.D.S, and B.L.P. wrote the manuscript with input from all coauthors.

Additional information

529   Supplementary information is available in the online version of the paper. Reprints

530   and permissions information is available online at www.nature.com/reprints.

531   Correspondence and requests for materials should be addressed to B.L.P.

Competing financial interests